Design of a Miniature Cone Penetrometer

Design and Calibration of a Miniature Cone Penetration Test Device for the Geo-Technical Centrifuge of Delft University of Technology

by

Siavash Honardar

in partial fulfilment of the requirements for the degree of
Master of Science
at the Delft University of Technology,
to be defended on December 11, 2019.

Student number:	4291255
Project duration:	September 1, 2019 – November 20, 2019
Thesis Supervisors:	Dr. A. (Amin) Askarinejad
	Ir. D.A. (Dirk) de Lange

Delft University of Technology
Faculty of Civil Engineering and Geo-Scinces
Master Applied Earth Sciences

TU Delft | Delft University of Technology | Faculty of Civil Engineering and Geo-Sciences | Master Track Geo-Engineering

Preface

This report serves the purpose of outlining a design proposal and research done by a student from Delft University of Technology. The proposal is focused on the creation of a cone penetrometer for the Geotechnical Centrifuge of the university. Several experiments were also conducted in order to observe the behavior of such devices. This design proposal is a part of creating this device for future use of the university and further research.
Readers interested in obtaining more insight to design parameters of a miniature CPT and basic concepts of physical modelling can refer to the content of this progress report.
Delft, November 2019

Abstract

The aim of this project is to elaborate upon the design proposal of a miniature cone penetration test device. The usage of CPTs in the geotechnical centrifuges has proven to be a reliable experimental method. The usage of a CPT in a centrifuge can provide determinant results for many applications of geotechnical experimentation.

The usage of cone penetration tests in centrifuge modelling is a significant experimental method in geotechnical engineering. The measurement of cone resistance and pore-pressure during in-flight tests can provide valuable data to correlate with soil properties and material behaviour. Through the years, this method has proven to be reliable and repeatable and has helped in verifying correlations of laboratory measurements and field data. The inexpensive and time-efficient nature of centrifuge testing and the reliability of cone penetration testing complement each other. This method has many relevant applications and acts as an effective tool

A literature study is conducted to obtain practical information on the design process of miniature CPTs. The existing designs are studied and their specifics are compared to the boundary conditions of the centrifuge of Delft University of Technology. This apparatus is capable of conducting tests at 300 times the gravitational acceleration and can carry samples with widths up to 400 millimeters. Two sets of existing sample containers are considered in this project which define physical dimensional boundaries. These sample containers consist of rectangular and cylindrical boxes with defined dimensions. The existing boundaries are further analyzed with respect to boundary effects derived from previously conducted tests to define design specifications for a potential miniature probe.

The definition of such boundaries set the basis of the design proposal. For the rectangular containers a miniature probe with a maximum diameter of 4 millimeters can be used. As for the cylindrical sample containers, miniature probes with maximum diameters of 7.5 and 9.5 millimeters are appropriate to be designed. The analyzed existing designs are then scaled and altered with respect to the determined boundary values and the proposal is further evaluated.

Three miniature CPTs are designed with diameters of 4, 7.5 and 9.5 millimeters. Each design has certain applications and can be used in specific scenarios. All three designs include modular load cells and sub-parts that can be replaced and altered. Each proposed device consists of a modular load cell designed based on required material properties to experience a minimum amount of 500 micro-strain without buckling.

The first design, with a cone diameter of 4 millimeters, can be used in any container with a minimum width of 12 centimeters and for soil samples with a maximum average grain size of 200 micrometers. The second design, with a cone diameter of 7.5 millimeters, can be used in containers with a minimum width of 22.5 centimeters and is applicable to soil samples with a maximum average grain size of 270 micrometers. The final design, with a diameter of 9.5 millimeters, is meant to be used in sample containers of widths above 28.5 centimeters and for soil samples with a maximum average grain size of 340 micrometers.

The designs are then evaluated with regards to manufacturing costs and feasibility. An estimation is made based on previously designed and patented devices and material catalogues provided by manufacturers. The cost of the first two designs are estimated to amount to 1580 to 2080 Euros, whereas the third design is estimated to cost 3080 to 3580 euros due to temperature compensated pore-pressure sensor that is included in the design. Upon further evaluation, the first design with a diameter of 4 millimeters is chosen as the most feasible and practical concept due to applicability and practicality of the design.

Acknowledgements

I would like to thank Dr. A. (Amin) Askarinejad for his constructive assistance and guidance throughout this project. His presence and cooperation throughout the project has been helpful and is very much appreciated.
I would also like to thank Ir. D. A. (Dirk) de Lange without whom this project would have been much more difficult. His patient guidance and constant feedback has been constructive and is sincerely appreciated and valued.
I would lastly like to thank H. K. J. (Karel) Heller and Ing. C. (Kees) van Beek, who have offered a great amount of help with the technicalities of testing, conducting experiments and providing resources and constructive opinions on the subject matter.

Contents

List of Figures

List of Tables

1 Introduction

In modern day geotechnics, aspects such as feasible replication of field tests and appropriate means of parameter determination have proven to be increasingly significant. In that matter, the usage of centrifuges has been widely implemented into the practice of laboratory testing of geotechnical problems.

Centrifuge modelling of geotechnical problems is a prominent and significant form of physical modelling as it creates a platform for experiments to be conducted with less expenses and in a more time-efficient manner (Gui, Bolton, & Phillips, 1993). A cone penetration test, CPT for short, is a frequently used and reliable in-situ investigation technique in geo-engineering. Cone penetration tests have been a prominent testing method in centrifuge modelling with the aim to check the repeatability and uniformity of the tested soil (Gui & Bolton, 1998). Other applications of CPTs in centrifuge testing include, but are not limited to, replication of in-flight strength profiles (Gui & Bolton, 1998) and verification of correlations between cone resistance and soil properties (Mo, 2014).

The objective of this project is to illustrate the steps taken in designing miniature penetrometers for a geotechnical centrifuge. The existing centrifuge and available testing apparatus define physical boundary conditions that are necessary to implement in the proposal of a design. Boundary conditions and boundary effects act as limiting features and create constraints to the application of field-scale testing devices.

Several physical features such as probe diameter, sample container geometry, soil type and penetration rate act as defining factors when speaking of the design of a miniature penetrometer. These factors not only outline the physical properties and the geometry of the design, but also are influential with regards to the formulation of measurements.

The first chapter of this report illustrates the literature study done on cone penetration testing and fundamentals of physical modelling. This chapter then proceeds to discuss a number of existing designs, one of which was tested throughout this project. The following chapter focuses on the description of the testing facility and the existing experimental apparatus which are considered as boundary condition defining factors. Chapter 4 elaborates upon the design approach with regards to the defined boundary conditions. Chapter 5 of this report discusses and illustrates the proposed designs as the final result of this project. The designs are then analyzed and further evaluated in the following chapter and a cost estimation is presented. The seventh chapter of this progress report provides recommendations for calibration of a potentially manufactured device based on the designs provided. The report is then concluded in the final chapter and a series of recommendations are discussed for further development of such designs.

2 Literature Review

Cone penetration testing has proven to be one of the most significant forms of in-situ geotechnical investigation techniques. The applications of CPTs consist of determination and identification of soil profiles, interpolation of ground conditions and evaluation of engineering and experimental parameters of soils (Jacobs, 2004). Despite the fact that CPTs are one of the most effective investigation techniques, it is undeniable that correlation of certain properties based on measurements obtained through CPT testing, relies on a series of empirical factors that are derived through calibration and experimentation (Gui & Bolton, 1998). Such empirical methods such as usage of a calibration chamber were suggested to often result in unreliable outcomes. (Been & Crook, 1988). Other research has also shown that it is practically impossible to recreate in-situ conditions in calibration chambers (Elbrich, 1994).

Considering the fact that soil properties are stress-dependent and vary based on the history of the soil, conducting measurements in representative states is a crucial parameter in experimental testing. Obtainment of soil parameters in representative stress states can result in more accurate derivations of modelling parameters. As stress-states can be reproduced in laboratory testing, the question of achieving a representative soil state in which a CPT test can be conducted arises.

Such visions and questions have led to the development of miniature CPT cones to be used in centrifuge tests. Centrifuge modelling of geotechnical problems realizes the opportunity to avoid full-scale tests and to reduce expenses and time-constraints. Miniature cones have an outstanding impact on centrifuge modelling as they not only determine the uniformity of the sampled specimen, but also provide the necessary data from which the in-flight strength of the soil profile can be determined (Bolton et al., 1999).

This chapter aims to illustrate the literature research done on existing miniature cone penetration testing devices and to highlight the significant boundary conditions and relevant physical modelling laws. Such aspects are of great importance as they will directly influence the design to be proposed.

2.1 Cone Penetration Testing (CPT)

Cone penetration tests are conducted by pushing a cone into the ground at a constant rate. The result of the tests are meant to deliver continuous and intermittent measurements of the resistance of the soil against the lowering of the cone. The usual penetration rate in the field is 20 mm/s. (Lunne, Robertson, & Powell, 1997). The most general resultant measures from a CPT test consist of the cone resistance q_c, the sleeve friction f_s and often the pore pressure of the soil u. The usage of electric cone penetrometers in combination with load cells, compared to mechanical penetrometers, has proven to provide readings that are more accurate, specially in soft soils. The development of the Fugro electrical friction cone illustrated in Figure 1 set the standards for referencing test procedures (Lunne et al., 1997).

Different types of cone penetrometers have been designed and each different type has a wide range of applicability. The most common form is the subtraction cone load cell arrangement. This arrangement obtains the sleeve friction by subtracting the tip from the total load. The resolution of the obtained measurements through this method is however believed to be poor (DeJong, Frost, & Cargill, 2001). It is therefore more feasible if the two force entities are measured separately by using isolated load cells for each unit.

Several factors affect the measurements conducted by a CPT. The most significant and primary factors that are influential with regards to cone resistance and pore-pressure are majorly accounted for in the design of penetrometers (DeJong et al., 2001). The factors influencing sleeve friction are however more ambiguous and are a subject of research. The primary influential aspects consist of, but are not limited to, load cell design, material properties, surface roughness of the sleeve and positioning of physical units such as the sleeve itself.

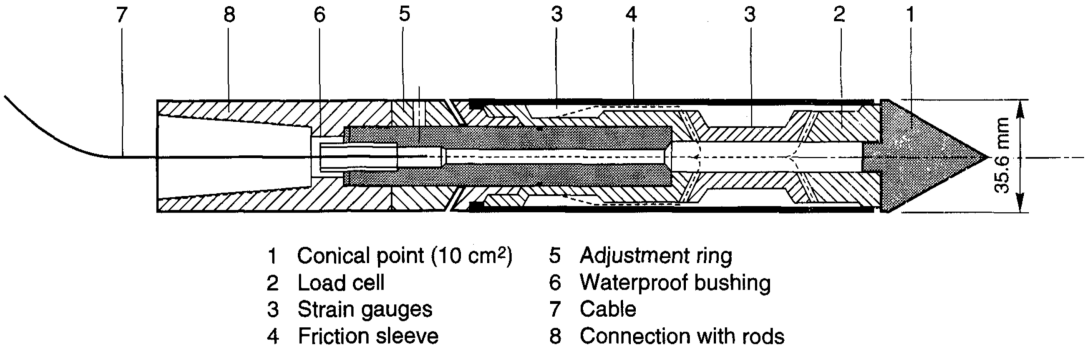

Figure 1: The Fugro Electrical Friction Cone.
Reprinted from Cone Penetration Testing in Geotechnical Practice, by Lunne et al. 1997t.

Figure 1 also illustrates the several parts to a standard CPT cone. These aspects and sub-parts are essential to proposing a design for a miniature CPT. Miniature CPTs have been developed in order to conduct and replicate tests in calibration chambers and centrifuges. Utilizing such miniature testing devices not only allows for down-scaling geotechnical scenarios, but also offers other advantages. These advantages consist of aspects such as lower thrusts necessary to advance the cone into the soil, possibility of identifying thinner lenses, usage of smaller driving mechanisms (Nikudel, S.E., Khamehchiyan, & Jamshidi, 2012) . The already existing miniature cones are to be discussed in section 2.5.

2.2 Centrifuge Testing and Physical Modelling of CPTs

Geotechnical modelling of soil behaviour is a complex matter as soils behave non-linearly and have stress/strain dependant behavioral tendencies. Centrifuge modelling of such problems enables the geotechnical engineer to replicate such complex features in an inexpensive and time-efficient way (Taylor, 1994). The process of down-scaling a field-size geotechnical problem into a small-scale model is the main essence of centrifuge modelling.

The reliability of CPTs in the centrifuge has proven that this method can act as a new alternative for soil parameter determination in representative stress states in a cost and time efficient manner (Mo, 2014). The usage of CPTs in centrifuge modelling is an important step in the verification of correlations between test results and soil properties.

2.2.1 Fundamentals of Physical Modelling and Scaling Laws

The main factor to be considered in physical modelling of geotechnical problems using centrifuge testing is the scaling laws. Such scaling laws are derived by utilizing dimensional analysis. The down-scaling of a field-model to a prototype in terms of geometry can be illustrated with respect to the ratio between their dimensions. Considering a model with dimension D_M and a prototype with dimension D_P, one can define a geometrical and modelling scale as follows;

$$\frac{D_M}{D_P} = \frac{1}{N} \tag{1}$$

Where N is the modelling scale. Application of this scaling procedure can be further illustrated with respect to stresses. Consider a situation illustrated in Figure 2, the subscripts M and P correspond with model and prototype respectively.

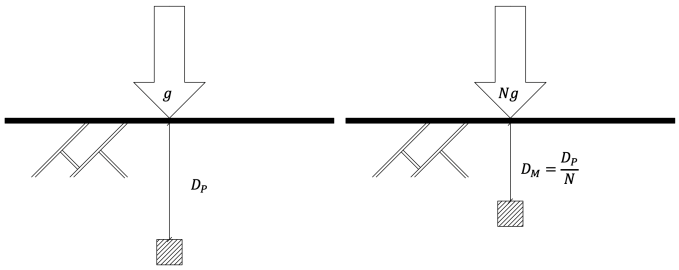

Figure 2: Stresses in Prototype vs Model

As it can be seen, the physical dimensions of the prototype are to be scaled down by a factor of N whereas the material existing in the prototype and the model are the same. The mentioned assumptions and arguments can be formulated as below;

$$D_M = \frac{D_P}{N} \tag{2}$$

$$\rho_M = \rho_P \tag{3}$$

The vertical stresses can be compared as follows;

$$\sigma_P = \gamma_P.D_P = \rho_P.g.D_P \tag{4}$$

$$\sigma_M = \gamma_M.D_M = \rho_M.Ng.D_M \tag{5}$$

Taking equations 2 and 3 into account and replacing the terms results in;

$$\sigma_M = \gamma_M.D_M = \rho_M.Ng.D_M = \rho_P.Ng.\frac{D_P}{N} \tag{6}$$

$$\sigma_M = \sigma_P \tag{7}$$

Therefore, as illustrated in equations 2 to 7, the stresses are equal once the scaling factor is taken into consideration with regards to all scaling quantities. The parameters involved in centrifuge testing of CPT's, can all be represented as equations consisting of physical quantities.These equations are dimensionally homogeneous and therefore can be reduced to a relationship among a complete set of dimensionless products (Wood, 2004). Relevant scaling laws for physical modelling in the centrifuge are summarized in Table 1(Konkol, 2014).

Table 1: Relevant Scaling Laws

Quantity	**Symbol**	**Scaling Factor: Model/Prototype**
Length	L	1/N
Displacement	u	1/N
Area	A	$1/N^2$
Volume	V	$1/N^3$
Strain	ϵ	1
Stress	σ	1
Force	F	$1/N^2$
Density	ρ	1
Mass	M	$1/N^3$
Acceleration	a	N
Velocity	v	1

2.2.2 Penetration Rate

As mentioned in section 2.1, the usual field penetration rate of a CPT is 20 *mm/s*. In order to replicate a field-test in the centrifuge, dimensional and physical entities regarding the test need to

be scaled and adjusted. However, as seen in the previous section, the scaling factor for velocity is *N/N=1*. This means that ultimately, a pure replication of a field-CPT test would require an actuator which enforces a penetration rate of 20 *mm/s*.

There are certain aspects regarding alterations of penetration rate that have direct and significant influence on the behavior of the tested sample. One of the most significant aspects to be considered is the behavior of the pore-fluid with respect to penetration rate. Alteration of penetration rate results in changes in the drainage patterns of the sample and also affects the measured cone penetration parameters (Poulsen, Nielsen, & Ibsen, 2013).

Depending on the soil type that is tested, cone resistance and pore pressure patterns change when different penetration rates are applied. It has been proven that for sandy soils, the standard penetration rate of 20 *mm/s* appears to create a fully drained condition in the sample. In clay-rich soils however the same rate results in undrained conditions. In silty soils it was concluded that with decreasing penetration rates, higher values of cone resistance were resultant (Poulsen et al., 2013). Lowering the penetration rate allows for the pore-fluid to drain, resulting in different pore-pressures and cone resistance measures. The effect of penetration rate is further discussed in section 2.4.4.

2.3 Formulation of Measurements

Both penetration depth and cone resistance are to be normalized with respect to existing boundary conditions. The cone resistance is normalized with respect to the vertical stresses (σ_v and σ'_v), whereas the penetration depth is normalized with respect to the cone diameter (B). Normalization of tip resistance accounts for the effect of overburden stresses. This is due to the fact that the resistance of the soil is stress-state dependent (Lunne et al., 1997). The normalized cone resistance Q and penetration depth Z are obtained as follows (Bolton et al., 1999):

$$Q = \frac{q_c - \sigma_v}{\sigma'_v} \tag{8}$$

$$Z = \frac{z}{B} \tag{9}$$

Where σ_v is the total stress,σ'_v is the effective stress and z is the measured penetrated depth.

The radial acceleration field in a centrifuge is proven to result in non-linear trends in stress variations with depth (Schofield, 1980). Therefore, the measured depth of penetration for the prototype is to be transformed to a corrected depth as follows:

$$z_p = Nz(1 + \frac{z}{2R}) \tag{10}$$

Where z is the penetration depth, R is the radius of the surface to the center of the tested sample and N is the acceleration multiplication factor (Bolton et al., 1999). Another influential factor is the penetration rate or velocity which is to be normalized with respect to the applied penetration rate and probe size. The normalized velocity V is obtained as follows (Jaeger, DeJong, Boulanger, Low, & Randolph, 2010);

$$V = \frac{vB}{c_v} \tag{11}$$

Where v is the rate of penetration, B is the penetrometer diameter and c_v is the coefficient of consolidation.

2.4 Boundary Effects in Centrifuge Testing of CPTs

Consideration of boundaries and physical specifications of the test apparatus is a crucial step in physical modelling. This section aims to illustrate the different boundary effects with respect to different limiting physical aspects.

2.4.1 Ratio of Container Width to Cone Diameter

The dimensions of the container in which the sample is prepared for testing are significant. The inner width or diameter of the container is a limiting factor as the inner walls of the container may affect the obtained readings due to stress propagation and other effects (Gui & Bolton, 1998). The effects of these dimensions were studied in order to obtain a ratio that would define an appropriate window for dimensional limitations. The study was conducted on sand samples with dry densities of 1415 and 1681 kg/m^3 as minimum and maximum respectively. The densities of the specimens were obtained according to the container volume. The window of sample density used to obtain the effect of container width varies between 1613 to 1631 kg/m^3 (Gui & Bolton, 1998). The relative densities of the mentioned samples varies between 74% to 81%.

The ratio of container diameter D to cone diameter B should not fall under a measure of 30. The limiting state of D/B=30 is still resultant in very minor boundary effects. Some sources suggest that a D/B ratio of 40 is more appropriate (Gui & Bolton, 1998).

$$\frac{D}{B} \geq 30 : \text{With minor boundary effects} \tag{12}$$

$$\frac{D}{B} \geq 40 : \text{With no boundary effects} \tag{13}$$

2.4.2 Ratio of Insertion Depth to Cone Diameter

The insertion depth with respect to cone diameter also creates boundary effects. Through experiments, it has been observed that the tip resistance measures cannot be registered correctly at initial contact (Gui & Bolton, 1998). Obtainment of a ratio between penetration depth and cone diameter illustrates the measure of penetration at which full resistance of a soil layer can be registered. Pullout tests can be conducted during which a penetrometer is pulled out of the specimen after the completion of a penetration test in the centrifuge. Results of such tests illustrate that a ration of at least 5 is required for the device to register the full resistance (Gui & Bolton, 1998). The insertion depth effect is dependent on the density of the sample and the ratio to probe size for full registration of soil resistance may vary depending on this factor.

$$\frac{\Delta z}{B} \geq 5 \tag{14}$$

2.4.3 Grain Size Effect

Multiple experiments have been conducted in order to observe the effect of grain size on cone resistance with respect to the probe diameter (Mo, 2014). The interval in which the ratio of B/d_{50} is of negligible effect is dependent on the nature of the soil sample. For instance, for fine materials, it has been observed that cone resistance is not affected by grain size for ratios larger than 28. For coarser materials however, it has been observed that the effect is more or less negligible for ratios larger than 20 (Gui & Bolton, 1998). The ratio also has an effect on the shaft friction of piles and therefore, also has an effect on the sleeve friction of a CPT. The effect was discovered to . be negligible for ratios higher than 28 to 90 (Fioravante, 2002). Assigning these limiting ratios is highly dependent on the nature of the soil sample as factors such as grain geometry, roughness and relative density may affect the measurements as well. The boundary conditions caused by the grain size effect are summarized in equations 15 and 16. The average grain size of the samples used to determine these relationships is 0.22 mm.

$$\frac{B}{d_{50}} \geq 20 \tag{15}$$

$$\frac{B}{d_{50}} \geq 28 \tag{16}$$

The boundary defined in equation 15 is sufficient when only measuring cone resistance. If sleeve friction is to be measured, the criterion defined in equation 16 must be used.

2.4.4 Penetration Rate Effect

The effect of penetration rate on cone resistance have been observed in sand-kaolin mixtures and have illustrated different effects based on the state of the soil sample. It has been observed that the normalized cone resistance Q, tends to decrease as normalized velocity V increases in the range of 0.01 to 160 (Jaeger et al., 2010). As mentioned previously in section 2.2.2, increase of penetration rate not only alters shear conditions, but also affects the drainage nature of the sample.

It was observed that in sand-kaolin mixtures, a normalized velocity of less than 0.01 resulted in drained conditions. However several limit states were defined for different samples to react under undrained conditions. It is suggested that for a normally consolidate or lightly over-consolidated samples, undrained conditions arise for Normalized velocities higher than 100 (Schneider, Lehane, & Schnaid, 2007). The lowest minimum boundary value of normalized velocity for undrained conditions to arise was found to be 20 (Jaeger et al., 2010).

As it can be seen in equation 11, the normalized velocity is dependent on the coefficient of consolidation. Considering the fact that the consolidation time in centrifuge testing is scaled with a factor of N^2 (Konkol, 2014), the effect of this time factor is significant with respect to applied velocities. In order to counter-balance the consolidation time effect with respect to penetration rates, one may consider the alternation of the viscosity of the pore-fluid in the sample.

2.5 Existing Designs

Several centrifuge centers have designed testing apparatus for conducting in-flight cone penetration tests using miniature probes. These developed devices are of different sizes and are tested in different conditions. Some of the existing probes are elaborated upon in this chapter with the aim to illustrate the basis of the design to be proposed.

2.5.1 EPIC: European Programme of Improvement in Centrifuging

The EPIC program consisted of five European centrifuge centers as a collaborative effort to create miniature probes and improve the testing procedure. The five laboratories developed a miniature CPT device each and tests were conducted to compare the variations and consistencies of the tests (Bolton et al., 1999). A summary of the designs is illustrated in Table 2 where "R" and "C" are indicative of rectangular and circular container types.

Table 2: Test Configurations of the EPIC Program.
Adapted from Bolton et al.,1999

Laboratory	**Container** $[mm]$	**Cone Diameter** $[mm]$	**Radius to Surface**$[mm]$
CUED Cambridge University Engineering Department	C: 210,850	10	3755
DIA Technical University of Denmark	C: 530	12	2295
ISMES Instituto Sperimentale Modelli e Strutture	C: 400	11.3	1840
LCPC Laboratoire Central des Pontes et Chaussées	R: 1200 × 800	12	5117
RUB Ruhr Universität Bochum	C: 100,750	11.3	3780

The devices illustrated in Table 2 are capable of measuring cone resistance. Most of the boundary effects in section 2.4 are based on the results obtained through tests conducted by this collaboration. The ultimate outcome of this collaborative effort illustrated that conducting in flight CPT tests is a reliable method of analysis and parameter determination. The consistency and repeatability of the resultant patterns and outcomes proves that miniature cone penetration devices are a legitimate and useful tool in geotechnical modelling (Bolton et al., 1999).

2.5.2 LEAP: Liquefaction Experiments and Analysis Projects

The LEAP project is a collaboration with the aim of validating numerical models predicting soil liquefaction. As a part of this project, several centrifuge experiments were conducted at multiple facilities. As a measure of quality control, in flight CPT tests were conducted to monitor and evaluate the sample densities (Carey et al., 2018).

Therefore, a miniature cone penetration device was designed with a diameter of 6 *mm*. This device is capable of measuring cone resistance and includes a load cell attached and screwed to a coupling of solid and hollow rods. The tip is threaded into the inner rod and the effective length of the device is 100 *mm*. The sealing of this rod was ensured by the usage of O-rings.

2.5.3 Other Designs

Other miniature CPTs have been developed for specific applications in different facilities. Some of these devices are presented in order to further elaborate the application of CPT testing in centrifuges.

An instance of such designs includes the development of a half probe by Mo(2014) from the University of Nottingham. This half probe has a diameter of 6 *mm* and is attached to a guiding bar with a width of 5 *mm*. There are a series of strain gauges located at the tip, 200 *mm* from the tip and at the end of the rod. The entire rod is then connected to a load cell. The effective length of this device is 300 *mm* (Mo, 2014).

Another example of other designs is a series of penetrometers developed by Kim et al. (2013) (Kim, Kim, Kim, & Choo, 2013). These device utilizes the usage of strain gauges with a detachable cone tip. The CPTs were developed to further investigate size effects and boundary effects for centrifuge testing. Miniature cones of different diameters namely 7, 10 and 13 *mm*, were developed and tested. The mentioned devices were only capable of measuring cone resistance.

As a final example, another CPT was developed by Ghayoomi et al. (2018) (Ghayoomi, Jarast, Mirshekari, & Borghei, 2018). This cone is 12.7 *mm* in diameter and includes a porous filter with an exterior pore-pressure transducer. The cone is connected to a load cell, making it possible to measure cone resistance and pore-water pressures (Ghayoomi et al., 2018).

2.5.4 Deltares ø8 mm Miniature CPT

The Deltares miniature cone of ø8 *mm* is another example of miniature cone penetration test devices developed in the past. This device was designed in the year 2000 and is capable of measuring up to 250 *N* of reaction forces. A rough detailing of this cone is illustrated in Figure 3. This cone was made available to this project and was tested using the TU Delft centrifuge actuator. The results and calibration of this cone are illustrated in Appendix 1.

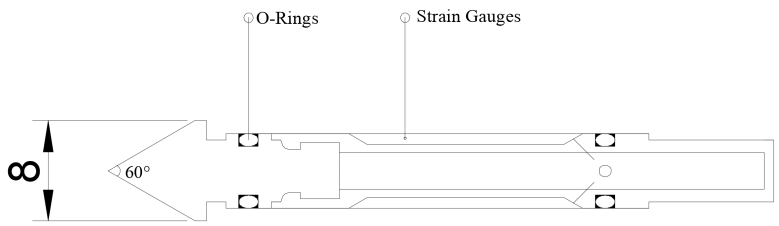

Figure 3: Rough Detailing of the Deltares Mini-Cone (Dimensions in [*mm*])

3 Modelling Methodology and Existing Apparatus

The existing apparatus at the Delf University of Technology, consisting of the entire centrifuge system and the sample containers, define certain boundary conditions. This chapter outlines the specifications and relevant boundary conditions dictated by the centrifuge and sample containers.

3.1 Specification of the TU Delft Centrifuge

The geotechnical centrifuge of the Delft University of Technology (TU Delft) is located at faculty of Civil Engineering and Geo-sciences. This device has a diameter of 2440 millimeters and has the functional capacity of being tested at 300 times the gravitational acceleration (Alderlieste, Dijkstra, & Tol, 2011). A schematic of this centrifuge is illustrated in Figure 4.

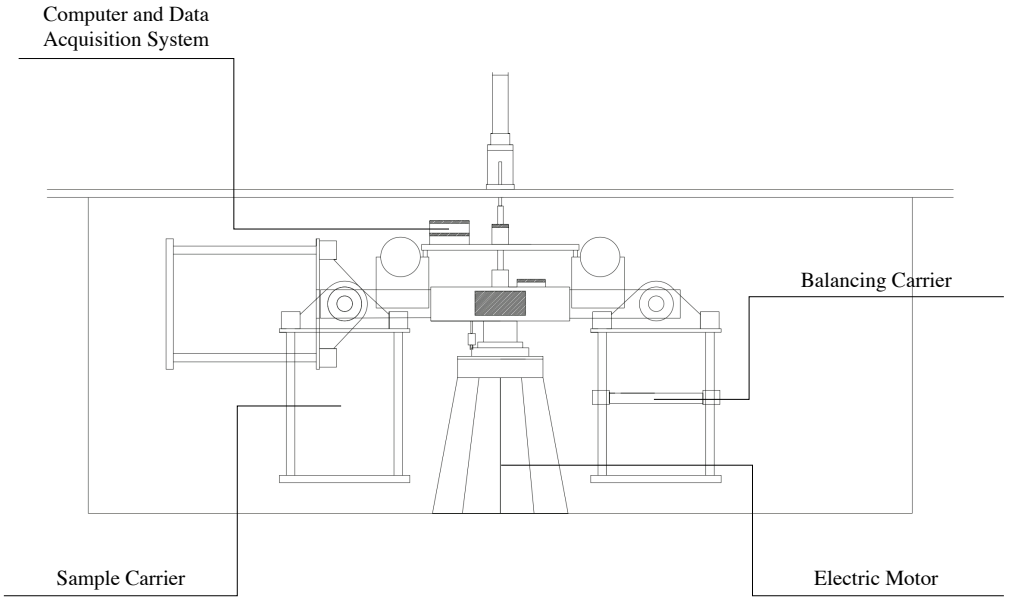

Figure 4: Geotechnical Centrifuge, TU Delft
Adapted from Experimental Investigation Into Pile Diameter Effects of Laterally Loaded Mono-Piles, by Alderlieste et al. 2011.

As illustrated in Figure 4, a computer and data acquisition system is mounted on the main frame. With this system the actuator of the centrifuge can be controlled using which, lateral and vertical displacements can be controlled (Alderlieste et al., 2011). The specifications of this centrifuge are summarized in Table 3. The physical boundary conditions and loading conditions are further discussed in sections 3.2 and 3.3.

Table 3: Specifications of the TU Delft Centrifuge

Element	Quantity	Unit
Maximum Sample Size	$300 \times 400 \times 450$	mm^3
Centrifuge Arm Radius	1220	mm
Maximum Design Acceleration	$300g$	m/s^2
Maximum Design Payload at $300g$	40	kg
Carrier Dimensions	$500 \times 240 \times 380$	mm^3

3.2 Dimensional Boundary Conditions

Aside from the carrier dimensions and maximum sample size mentioned in Table 3, the containers often used in the TU Delft centrifuge have defined specifications. There are currently two existing models of containers which define the dimensional boundary conditions. Figure 5 and 6 illustrate the geometry of each container. The illustrated dimensions are not necessarily exact as not all the existing containers have the same geometry. It is also important to consider the fact that these containers have been used in other simulations and may be slightly deformed.

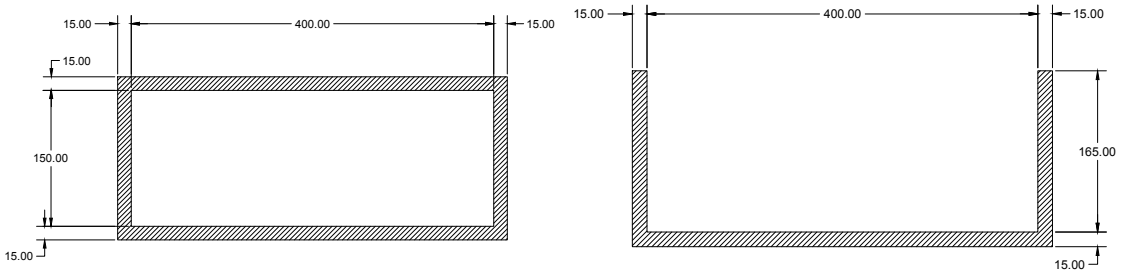

(a) Top Profile Rectangular Container (b) Cross Section Rectangular Container

Figure 5: Rectangular Container (Dimensions in $[mm]$)

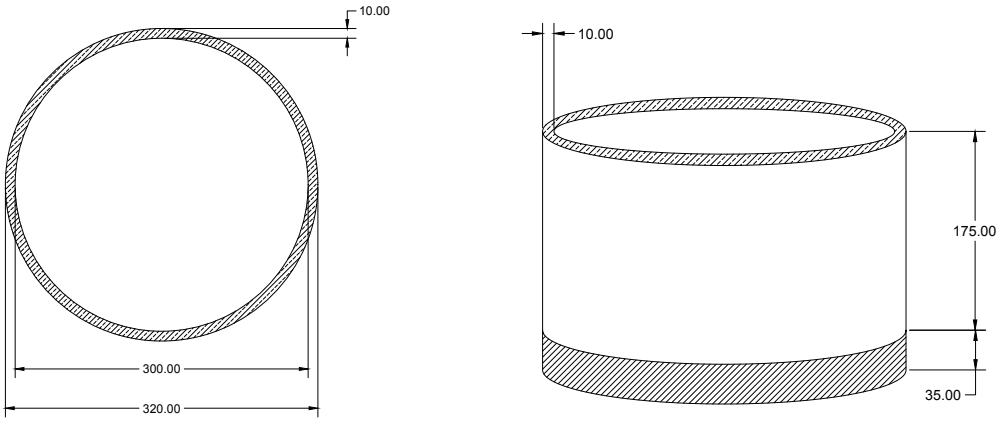

(a) Top Profile Cylindrical Container (b) Side Profile Cylindrical Container

Figure 6: Cylindrical Container (Dimensions in $[mm]$)

The dimensions and geometry of these containers define the physical boundary conditions mentioned in section 2.4. The specifics of each container are summarized in Table 4. The indicated dimensions and their effect on the proposal of a design will be further discussed in section 4.2.

Table 4: Specifications of the Used Sample Containers

Container Type	**Inner Dimensions** $[mm]$	**Outer Dimensions** $[mm]$
Rectangular Container	$165 \times 150 \times 400$	$180 \times 180 \times 430$
Cylindrical Container	$\text{ø}300 \times 175$	$\text{ø}320 \times 210$

3.3 Boundary Conditions with regards to Loading Frame and Actuator

The current actuator and loading system utilized in the TU Delft centrifuge have certain limitations. The maximum loading range of the currently installed actuator is 3.3 to 3.5 kN and the maximum driving velocity is 0.1 mm/s. These limitations can be further investigated in order to define more flexible boundary conditions with regards to loading and penetration rate.

The current limitations are confined to the bending stiffness of the loading frame and the design of the actuator itself. Altering such designs and utilizing measures to ensure the prevention of deformations may improve test results.

4 Design Approach

4.1 Comparison of Existing Options

The designs described in section 2.5 are compared to set the basis of the design proposal. Aside from this comparison, certain demands are to be met with regards to the measuring capabilities of the proposed design. The choice was made to approach the design process with creating possibilities for cone resistance, sleeve friction and pore-water pressures to be measured.

The designs discussed in section 2.5 are summarized in Table 5 in order to illustrate the differences and similarities.

Table 5: Design Comparison

Design	q_c	f_s	pore-pressure	Relevancy to Design Approach
EPIC	✓	×	×	Moderate Relevancy
LEAP	✓	×	×	High Relevancy
Mo, 2014	✓	×	×	Low Relevancy
Kim et al., 2013	✓	×	×	High Relevancy
Ghayoomi et al., 2018	✓	×	✓	Moderate Relevancy
Deltares ø8 *mm*	✓	×	×	High Relevancy

The most relevant designs were taken into consideration during the design process. Upon availability of technical drawings, the most relevant designs along side other designs of field-size CPT's were scaled and recomposed in order to create a basis for the designs to be proposed.

4.2 Approach with regards to Boundary Conditions

The boundary conditions defined in the previous chapters outline defining features for the proposal of a design. These features are outlined in order to set pre-conditions for the design proposal.

As mentioned in section 2.4.1, the ratio of the sample container width to probe size is of significance when analyzing boundary effects. Considering the conditions mentioned in section 2.4.1 and 3.2, an approach can be taken with regards to the diameter of the probe to be designed. The maximum probe size with regards to the size effects defined in section 2.4.1 and the container sizes can be defined as follows.
Rectangular container with $D = 150\ mm$ and a minimum ratio of 40;

$$\frac{D}{B} \geq 40 \rightarrow B \leq 4mm \tag{17}$$

Cylindrical container with $D = 300\ mm$ and ratios of 30 and 40;

$$\frac{D}{B} \geq 30 \rightarrow B \leq 10mm \tag{18}$$

$$\frac{D}{B} \geq 40 \rightarrow B \leq 7.5mm \tag{19}$$

As it can be seen in equations 17 to 19, the diameter of the penetrometer needs to be less than 4 *mm* for the rectangular container and less than 7.5 *mm* for the cylindrical container. A diameter smaller than 10 *mm* is also acceptable for the cylindrical container as it will only result in minor boundary effects. Considering the mentioned conditions, a design proposal can be formed for 3 different CPT probes. The proposed diameters are 4, 7.5 and 9.5 *mm*. The proposed dimensions are further analyzed in the following section.

4.3 Limitations and Prerequisites

Considering the diameters that are decided upon, already existing devices can be scaled down to miniature versions. However, simple geometrical scaling of CPT rods is not feasible as details such as wire-space or sensor chambers cannot be linearly scaled. Certain limitations are therefore influential when proposing such designs. One of the most significant limitations is the size of a temperature-compensated pore-pressure transducer that can be used in the design. Such a sensor is at least 6 mm in diameter and 10 mm in length. This transducer can only be implemented in the last design which is 9.5 mm in diameter. There are however other pore-pressure sensors that may not be temperature compensated with smaller dimensions. Such transducers can be implemented in the design with a diameter of 7.5 millimeters. The dimensions define limitations as to how many sensors can be placed in the device and therefore each of the proposed designs have pre-defined functionalities. Each proposed design is further discussed in the following chapter.

4.4 Design of Physical Parts

It is important to define specific dimensions for each physical unit of the device. The governing factor with regards to this approach is the analysis of Euler's critical load criteria. The designs must contain a hollow outer tube of a certain diameter. The stiffness of the material used to manufacture this outer rod must be high enough to prevent the entire device from buckling.

Uniform hollow cylinders are available in different dimensions and can be made from a wide range of materials. In order to avoid any damage to the device, the material type is chosen as rust free stainless steel, specifically AISI-304. This steel type has a Young's modulus of 200 GPa at room temperature. Since the diameters of the designs are defined, it is possible to choose the dimensions of the outer rod. Rods with dimensions of $ø4 \times 0.5mm$, $ø7.5 \times 0.5mm$ and $ø9.5 \times 0.5mm$, are available in the form of a uniform hollow cylinder (Salomon's Metalen B.V., 2016). The chosen material type of AISI-304 can withstand loads up to 6.03, 12.06 and 15.50 kN for each of the mentioned designs respectively.

The same steel type is used for the construction of the load cell, cone and the inner solid rod that attaches the cone to the load cell. The exact dimensions of the other units are specified in chapter 5.

4.5 Design of Load Cells

As previously noted, each design has a series of specific applications. The load cell arrangement and specifications define the scope of application for each design. It is also important to note the option of modularity of such load cells. The flexibility of removing and replacing the load cell for different experiments expands the scope of applications for each design. In order to design these load cells, each different application needs to be taken into consideration and categorized.

Three categories are chosen for expected cone resistances. Each of the categories corresponds to different soil materials. The three categories are summarized in Table 6. For each of the categories, a minimum measure of 500 micro-strains is defined for the load cell to experience. This limiting measure is defined to minimize noise and to have viable and reliable measurements. For each of the three categories, expected stresses and cross sectional areas are calculated with respect to defined material properties. As mentioned in the previous section, the material chosen for construction of the load cell walls is steel type AISI-304 with a Young's Modulus of 200 GPa.

Table 6: Cone Resistance Categories and Corresponding Material

Category	$\mathbf{q_c}$ $[MPa]$	**Corresponding Material**
1	0.5 - 2	Soft soils, loose to dense clay
2	5 - 25	Sandy soils, loose/dense fine sand to loose coarse sand
3	30 - 70	Coarse and dense soils

The geometry of the load cell must also be designed so that withstands the expected applied loads. Taking all the previously mentioned factors, a series of calculations are conducted to determine the dimensions, expected loads and corresponding strains experienced by the load cell in each design. The geometry is to be designed in such a way that the load cell experiences at least 500 micro strain without deforming due to critical loading. A summary of the load cell designs is illustrated in Tables 7, 8 and 9. In each table, the load cell tube geometry is illustrated alongside the expected loads and corresponding strains for each pre-defined category.

Table 7: Load Cell Design 1

Design 1	**øDiameter: 4** *mm*	**Load Cell Tube:** Diameter: 2.5 *mm*,Thickness: 0.1 *mm*
Category	**Expected Loads [MPa]**	**Corresponding Strains [micro-strain]**
1	8 to 35	42 to 167
2	80 to 420	420 to 2083
3	500 to 1200	2500 to 5833

Table 8: Load Cell Design 2

Design 2	**øDiameter: 7.5** *mm*	**Load Cell Tube:** Diameter: 4.0 *mm*,Thickness: 0.125 *mm*
Category	**Expected Loads [MPa]**	**Corresponding Strains [micro-strain]**
1	14 to 60	73 to 290
2	145 to 725	726 to 3629
3	870 to 2030	4355 to 10161

Table 9: Load Cell Design 3

Design 3	**øDiameter: 9.5** *mm*	**Load Cell Tube:** Diameter: 5.0 *mm*,Thickness: 0.15 *mm*
Category	**Expected Loads [MPa]**	**Corresponding Strains [micro-strain]**
1	8 to 35	77 to 310
2	80 to 420	775 to 3877
3	500 to 1200	4652 to 10855

As it can be seen, in all three designs, for the second and third loading category, the proposed tubes experience enough strain to comply with the minimum thresh-hold value of 500 micro-strain. This confirms that the chosen material is appropriate for the two categories. However, for soft soils such as clay, none of the designs are able to register the minimum 500 micro-strains. The loads in this category are simply too low and therefore another solution must be implemented.

In order to measure in softer soils with the designed load cells, the construction material needs to be less stiff. This is however not an optimal approach as the stiffness needs to be lowered to a measure of approximately 15 GPa for the load cell to register the minimum requirements. Such a low stiffness may result in creep behaviour and deformation of the load cell and is to be avoided. Therefore, a more feasible solution can be formed for testing in softer soils. Figure 7 illustrates a possible scenario where a bending load cell is used on the frame of the actuator. This load cell is attached and screwed to a hollow rod that is attached and screwed to the cone on one end, and screwed to the frame on the other.

The modular nature of the design serves the purpose of realising such solutions as the load cell can be replaced by a hollow rod that can be screwed to the solid units of the device. This rod can then push and bend the load cell, measuring cone resistance. This concept is a meant as a suggestive solution that can be altered in several ways. There are several types of bending load cells with different capacities which can be applied to this concept.

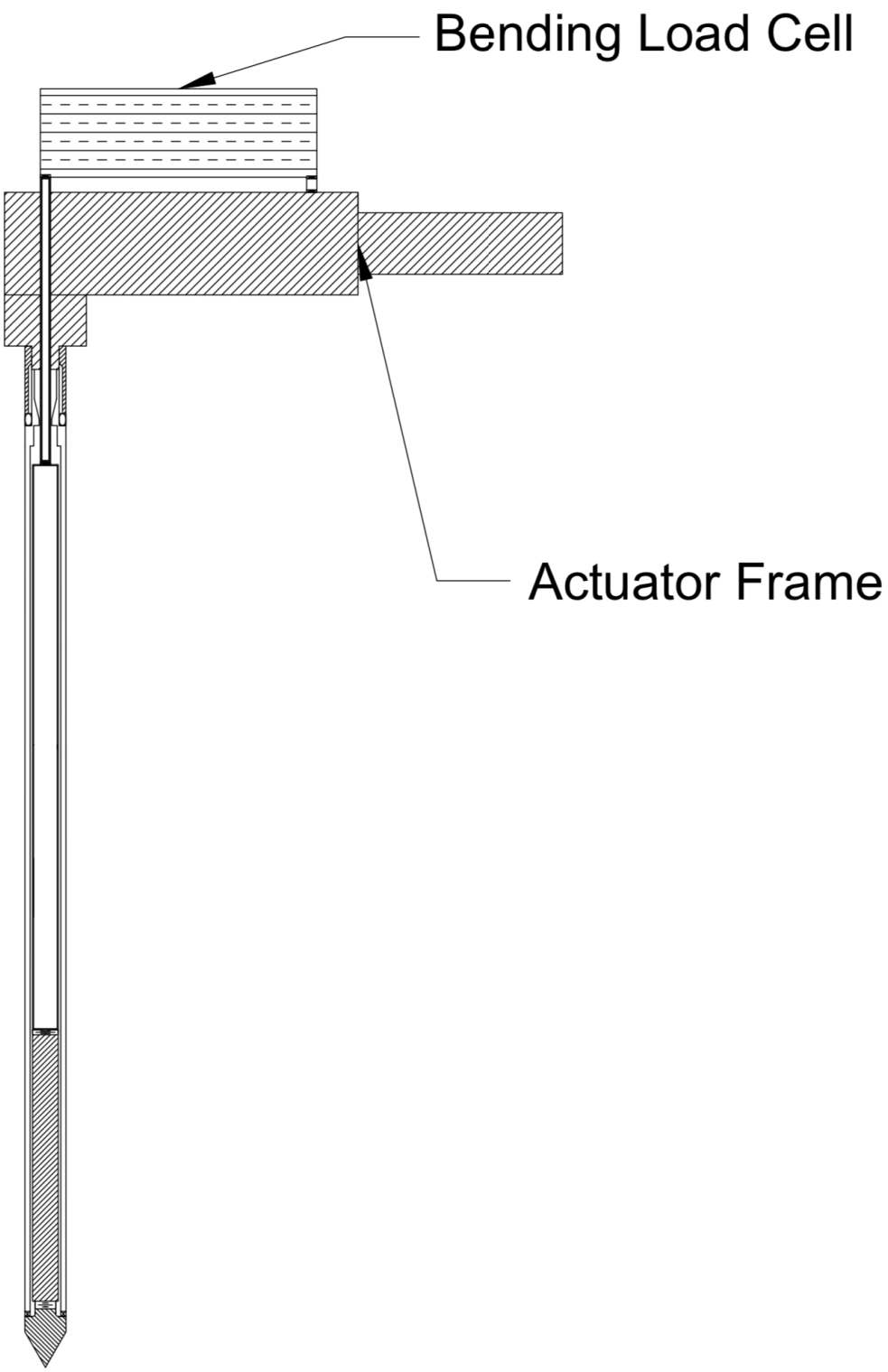

Figure 7: Testing Apartus for Soft Soils

5 Proposed Designs

This chapter concerns itself with the proposed designs based on the prerequisites defined in the previous chapters. Each design contains similar materials in terms of electronics and physicality. The designs are discussed in detail with regards to applicability in the following sections. The general detailing involved in the design process consist of different aspects which are illustrated and discussed per proposed design. A generalized design of the cone tip for the design proposals is illustrated in Figure 8.

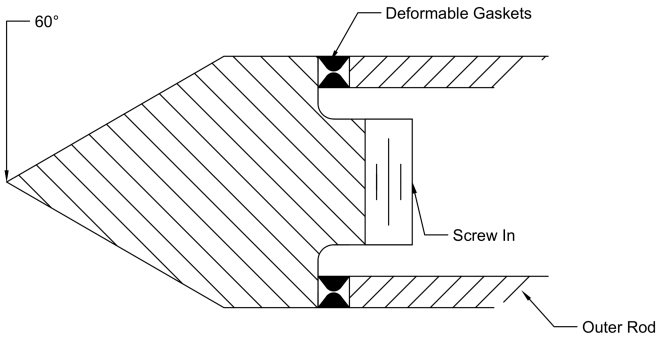

Figure 8: General Design of CPT Cone

As it can be seen in Figure 8, the angle of the cone is 60 °as the standard cone angle for field penetrometers (Lunne et al., 1997). The deformable gaskets illustrated in this figure are placed for sealing purposes. The screw in entity enables for users to attach the cone to other rods that act as modular parts of each design. For each design, the detailing of the cone is further illustrated in the following sections.

Another significant detail that is applicable to all designs is the usage of strain gauges. A general detail of a strain gauge is illustrate in Figure 9. As it can be seen, a defined amount of space is outlined for the strain gauge. This required space is not a physical entity but is a form of illustration to outline the placing of a strain gauge.

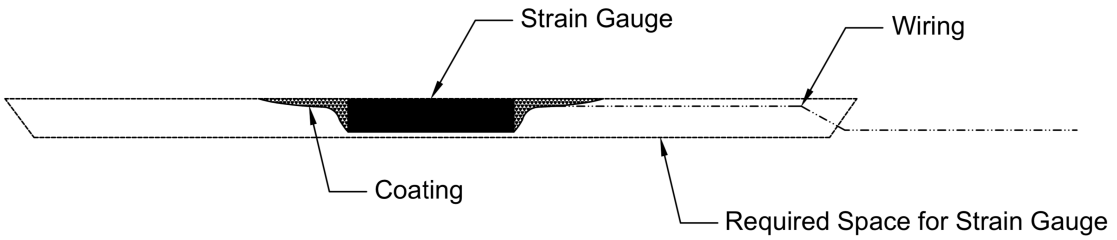

Figure 9: General Detail of Strain Gauge

Such strain gauges are used in load cells to measure the strain that a body is experiencing. As mentioned in the previous chapter, there are three designs with diameters of 4, 7.5 and 9.5 millimeters. Also mentioned previously is the fact that the load cells in the proposed designs consist of hollow cylindrical rods with strain gauges on the inner walls. In the previous chapter the general applicability of the specific load cell designs were illustrated. The designed load cells are illustrated per design in detail and the applicability of the device in its entirety is discussed.

5.1 Design 1: 4 mm ø; Measuring Cone Resistance

Figure 10 illustrates the first design with a diameter of ø4 mm. This design consists of a solid steel rod attached to the cone which is connected to a hollow rod with strain gauges acting as the load cell. The strain gauges used in this design are similar to Bolt strain gauges which are simply inserted into the tube and covered with glue. The outer tube is connected to the cone and is sealed using deformable gaskets.

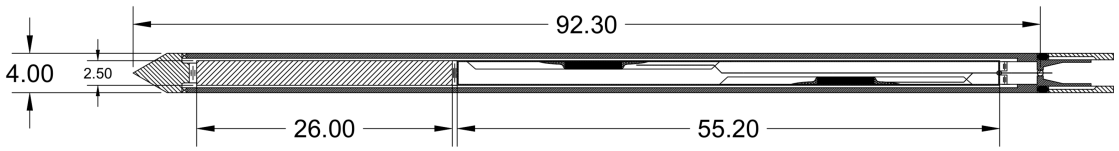

Figure 10: Design 1: 4 mm ø(Dimensions in $[mm]$)

This design is meant to be used in the rectangular containers mentioned in section 3.2. The dimensions are minimized to the extent that it can be used in several scenarios and boundary conditions.

5.1.1 Details: Design 1

The most significant details of this design are the cone and load cell. The two details are respectively illustrated in Figures 11 and 12.

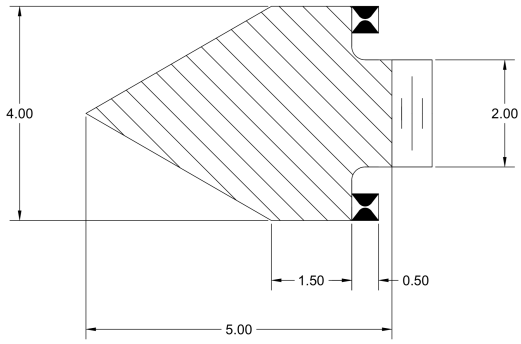

Figure 11: Cone Design 1 (Dimensions in $[mm]$)

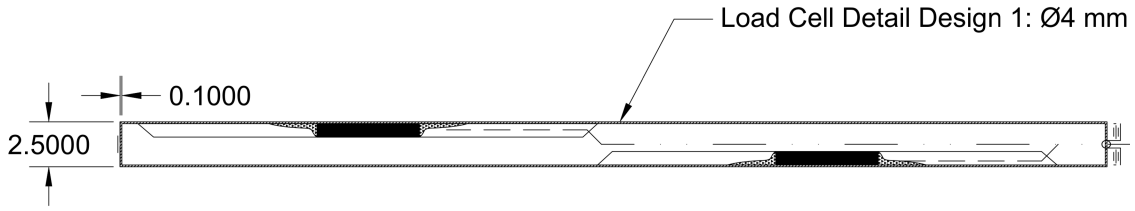

Figure 12: Load Cell Design 1 (Dimensions in $[mm]$)

As it can be seen, the load cell consists of a coupling of strain gauges back to back. The wiring is illustrated and the required space for the strain gauges is shown. Both ends of the rod can be screwed onto other units and the entirety of the contraption acts as a modular load cell. The

load cell only measures the strains generated by the forces translated from the cone to the rods attached to it. This device is only capable of measuring cone resistance.

5.1.2 Applicability and Load Cell: Design 1

The boundary effects with regards to the geometry of this device can be obtained by using the relationships illustrated in section 2.4. Using B=*4 mm* one can obtain;

$$\Delta z \geq 5 \times 4 \rightarrow \Delta z \geq 20\, mm \tag{20}$$

$$d_{50} \leq \frac{4}{20} \rightarrow d_{50} \leq 0.2\, mm \tag{21}$$

$$D \geq 30 \times 4 \rightarrow D \geq 120\, mm \tag{22}$$

Equations 20 to 22 illustrate the boundary conditions to which this cone can be applied to. As it can be seen, this cone can be used in containers with a minimum width or diameter of 120 *mm* and the average grain size of the sample must not exceed 0.2 *mm*. The cone is most likely to register the full resistance of the sample after a penetration depth of 20 *mm*.

This design can be used to its full potential in soil specimens with an expected cone resistance of at least 5 *MPa*. In order to utilize this device in softer soils, a solution similar to that introduced in section 4.5 can be used.

5.2 Design 2: 7.5 mm ø; Measuring Cone Resistance, Sleeve Friction and Pore-Pressure

Figure 13 shows the proposed design of the ø7.5 mm cone. This design consists of a solid cone with a porous disk, attached to a pore-pressure chamber. The cone contraption is attached to a solid steel rod which is screwed onto the load cell which translate the cone resistance forces. There is a sleeve tube with a coupling of strain gauges right behind the sleeve. This acts as the friction sleeve of the device. As mentioned in Chapter 2, it is best to separate the measuring load cells for cone resistance and sleeve friction and avoid subtraction load cell arrangements. This sleeve has a direct fixed connection with the outer rod and is 24 millimeters in length. The connection points between the cone and sleeve tube are sealed using deformable gaskets.

The wiring schemes are indicated with lines coming out of the sensor chambers and into the hollow tube. The wires are to have an exit from the end of the tube to the registering apparatus. The geometry of the device is designed in such a way to allow for wires of 0.5 *mm* in diameter to pass through the connection points. The pore pressure transducers for this design are not temperature compensated. This is a factor that must be kept in mind when testing at higher g-levels and when penetrating at higher penetration rates as more friction will cause higher temperatures.

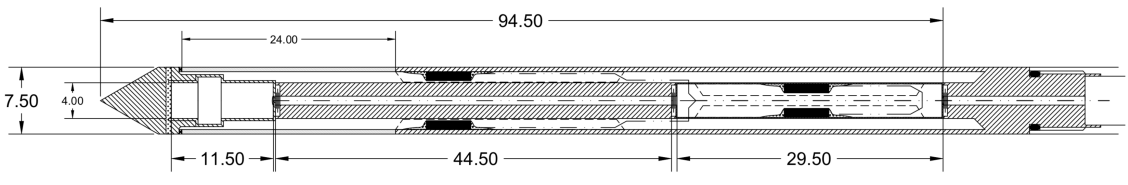

Figure 13: Design 2: 7.5 mm ø(Dimensions in [*mm*])

5.2.1 Details: Design 2

The cone contraption including the pore-pressure chamber is detailed out in Figure 14 where the dimensions and sub-parts of the unit are illustrated.

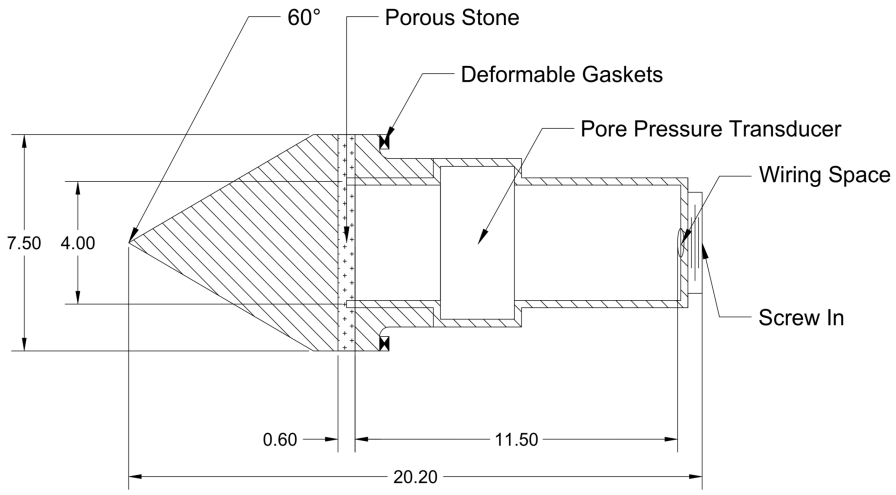

Figure 14: Cone Design 2 (Dimensions in $[mm]$)

Figure 15 illustrates the load cell detailing of this design. a set of strain gauges are placed on the inner walls of the tube with a wall thickness of 0.1250 *mm*. The required spacing of the strain gauges are highlighted as dashed lines and the wiring is shown as well.

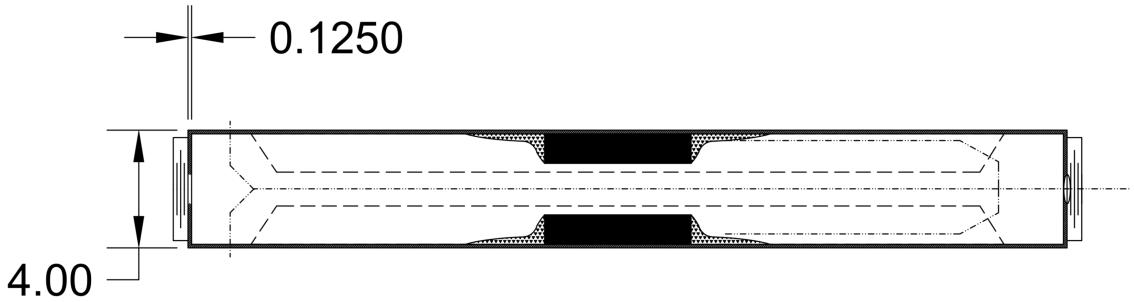

Figure 15: Load Cell Design 2 (Dimensions in $[mm]$)

5.2.2 Applicability and Load Cell: Design 2

Using B=*7.5 mm* the necessary boundary conditions can be defined as follows.

$$\Delta z \geq 5 \times 7.5 \rightarrow \Delta z \geq 37.5\, mm \tag{23}$$

$$d_{50} \leq \frac{7.5}{28} \rightarrow d_{50} \leq 0.27\, mm \tag{24}$$

$$D \geq 30 \times 7.5 \rightarrow D \geq 225\, mm \tag{25}$$

Equations 23 to 25 illustrate the boundary conditions to which this cone can be applied to. Therefore, this cone can be used in containers with a minimum width or diameter of 225 *mm* and the average grain size of the sample must not exceed 0.27 *mm*. The cone is most likely to register the full resistance of the sample after a penetration depth of 37.5 *mm*.

The design of the load cell makes the device appropriate for conducting tests in soils with a minimum expected cone resistance of 5 *MPa*. The friction sleeves are constructed from the same material as the rest of the device, that is steel type AISI-304.

5.3 Design 3: 9.5 mm ø; Measuring Cone Resistance, Sleeve Friction and Pore-Pressure

Figure 16 illustrates the design of the ø9.5 mm cone. This design is very similar to the previous proposal. The elements are exactly the same apart from the dimensions and the type of pore-pressure transducer. The sensor that is to be utilized in this cone is temperature compensated and is 6 *mm* in diameter. The outer tube is connected to the cone and is sealed using deformable gaskets.

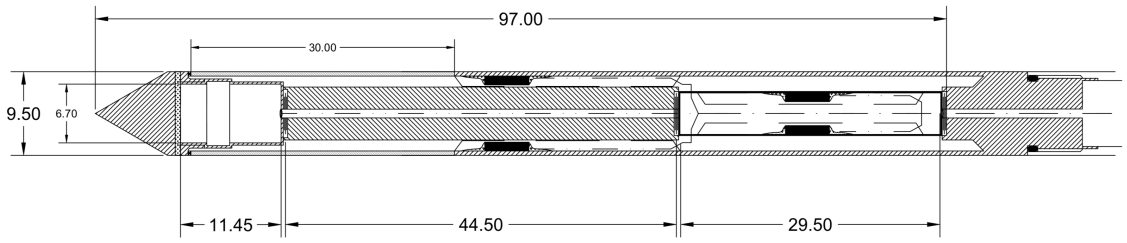

Figure 16: Design 3: 9.5 mm ø(Dimensions in [*mm*])

This design is meant to be used in the cylindrical containers mentioned in section 3.2. This is due to the fact that the probe size is too large for the rectangular containers and will result in large boundary effects.

5.3.1 Details: Design 3

Figure 17 illustrates the details of the cone for design 3. The dimensions and sub-parts are illustrated and are very similar to that of the previous design.

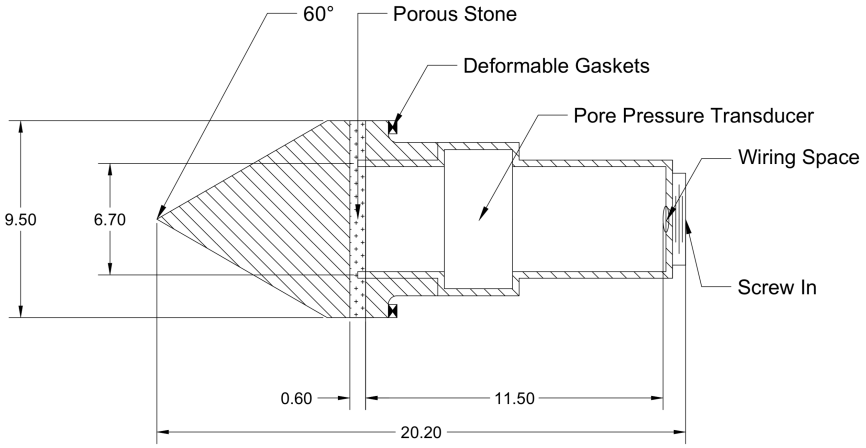

Figure 17: Cone Design 3 (Dimensions in [*mm*])

Figure 18 shows the load cell of design 3 with a wall thickness of 0.15 *mm* and a set of strain gauges on the inner walls. As it can be seen, the load cell is modular and can be screwed onto

other attachements.

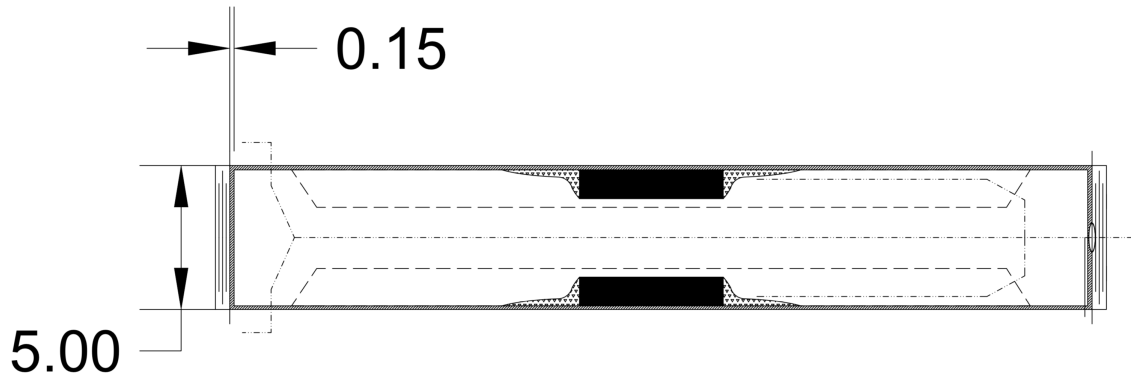

Figure 18: Load Cell Design 3 (Dimensions in [mm])

5.3.2 Applicability and Load Cell: Design 3

Considering the fact that the diameter of this cone is 9.5 mm, the boundary conditions can be defined as follows.

$$\Delta z \geq 5 \times 9.5 \rightarrow \Delta z \geq 47.5\, mm \tag{26}$$

$$d_{50} \leq \frac{9.5}{28} \rightarrow d_{50} \leq 0.34\, mm \tag{27}$$

$$D \geq 30 \times 9.5 \rightarrow D \geq 285\, mm \tag{28}$$

According to equations 26 to 28, this cone can be used in containers with a minimum width or diameter of 285 mm and the average grain size of the sample must not exceed 0.34 mm. The cone is most likely to register the full resistance of the sample after a penetration depth of 47.5 mm. The same scope of applicability with regards to soil types applies to this design as the ø7.5 mm design.

6 Analysis and Optimization

6.1 Cost Estimation

The proposed designs were evaluated by DEMO, Electronic and Mechanical Support Division of TU Delft, and a rough cost estimation was made for each proposed design. The estimation includes material costs, labour costs and the time duration for manufacturing the device. The most significant aspects of this estimation are summarized in Table 10. The rough total cost estimation for each design is summarized in Table 11

Table 10: Time and Cost Estimation of Manufacturing

Subject	**Description**	**Cost Estimate**	**Time Estimate**
Material: Tube	Stainless Steel AISI-304	€75 to 100	Delivery: 2 to 3 days
Labour Costs	Construction and Detailing	€1200 to 1300	1 Week of Effective Work
Material: Sensor	Strain Gauge	€10-20 p.p.	-
Material: Glue	Attachment of Strain Gauges	€10-15 p.p.	-
Material: Sensor	Pore-Pressure Transducer	€1500 p.p.	-
Labour Costs	Electronic Work	€500	1 Week of Effective Work

Table 11: Cost Estimation

Design	**Total Cost Estimation**
Design 1: ø4 *mm*	€1580 to 2080
Design 2: ø7.5 *mm*	€1580 to 2080
Design 3: ø9.5 *mm*	€3080 to 3580

The cost estimations above are only representative if the device is to be manufactured by DEMO. Other manufacturing units such as A.P. van den Berg can provide the same services at different costs. Information on manufacturing costs at other providers is dependent on their company policies and is therefore not precise.

6.2 Most Feasible Design

Upon further evaluation of the proposed designs, the first design with a diameter of 4 *mm* is seemingly the most feasible concept. This device can be applied in different scenarios and offers less limitations in terms of physical and dimensional boundary conditions. The design is flexible due to the modularity of the load cell and other physical units. This modular nature results in convenience and expansion of possibilities in centrifuge testing.

7 Calibration and Minimization of Boundary Effects

This chapter aims to provide suggestions with regards to the calibration of the manufactured designs and the minimization of the boundary effects.

7.1 Calibration

Analysis of results obtained through series of calibration chamber tests indicate a relationship between the cone resistance and the vertical effective stress (Jamiolkowski, Presti, & Manassero, 2001). It has been proven that the ratio of cone resistance to the square root of the vertical effective stress is meant to be nearly constant.

$$k = \frac{q_c}{\sqrt{\sigma'_v}} \approx constant \tag{29}$$

In order to achieve and ensure that this condition holds, the device can be tested in either a calibration chamber or the centrifuge itself. Applying a known load on the cone and placing a compressible prop under the cone will result in measurements with which this relationship can be observed.

7.2 Minimization of Boundary Effects

The most significant boundary effect that might affect the measurements is the effect of container size. For instance if the ø9.5 mm was to be used in a container with a width less than 280 mm, the measurements will be affected by the boundary effects related to the D/B ratio.

Such effects can be minimized by utilizing a rubber membrane covering the interior walls of the container. Such membranes can act as absorbing agents for boundary effects as they reduce the distortion of stress and strain fields (Coelho, Haigh, & Madabhushi, 2003). The choice of the insertion point must be centralized in order to avoid such boundary effects.

8 Conclusion and Recommendations

To conclude, the objective of this progress report was to act as a design proposal for a miniature cone penetration test device for the geotechnical centrifuge of TU Delft. The proposed designs are based on different factors such as boundary conditions, material properties and existing experimental apparatus.

Several existing designs were analyzed in order to understand the functionality of a miniature CPT. One available design was tested using the available experimental apparatus to further understand the performance of miniature penetrometers. Elements such as normalization of measurements and corrections of data collected with respect to the geometry of the CPT were also taken into consideration. The boundary effects caused by a miniature penetrometer were analyzed and separated into different categories. These categories include the effect of sample container geometry, the effect of insertion depth, the effect of average grain size and the penetration rate at which the device is inserted into the sample.

With respect to the boundary effects and limitations, a proposal was made for three separate designs, each with specific applications. The most influential factor is the container geometry. Based on the two available container types at the facility, with widths and diameters of 150 and 300 millimeters, diameters of 4, 7.5 and 9.5 millimeters were proposed for the designs. Limitations such as material properties and sensor types were taken into consideration and applied to the design of load cells for each proposed diameter.

The proposed designs have specific scopes of applicability. Design 1 with a diameter of 4 millimeters can be used in containers with a minimum width of 120 millimeters and in samples with a maximum grain size of 0.2 millimeters. This device is only capable of measuring the cone resistance. The second design with a diameter of 7.5 millimeters measures cone resistance, sleeve friction and pore-pressures and can be used in sample containers with a minimum width of 225 millimeters. The device is appropriate for experimentation in soil samples of a maximum grain size of 0.27 millimeters and soil types that have a minimum expected cone resistance of 5 MPa. The final design, with a diameter of 9.5 millimeters is similar to Design 2 but utilizes a temperature-compensated pore-pressure transducer. This design can be used in containers with a minimum width of 285 millimeters and in samples with a maximum average grain size of 0.34 millimeters.

A series of cost estimations were conducted to roughly assess the feasibility of the proposal and upon further evaluation the first design, with a diameter of 4 millimeters, was chosen as the most attainable and practical device for the existing centrifuge. This probe is flexible due to the modular nature of the physical entities that act as sub-parts to the design.

It is recommended to further analyze the performance of friction sleeves with regards to the arrangement of the load cell and strain gauges dedicated to the measurement of sleeve friction. The complexity of this aspect arises from the variability of the measurement and aspects such as design surface roughness. The process of approaching the design of a miniature cone penetrometer has proven to involve a wide range of complexities and is therefore a subject of further research and improvement.

References

Alderlieste, E., Dijkstra, J., & Tol, F. (2011). Experimental investigation into pile diameter effects of laterally loaded mono-piles. (Vol. 7). doi:10.1115/OMAE2011-50068

Been, K., & Crook, J. (1988). A critical appraisal of cpt calibration chamber tests. *Proc. Int. Symp. on Penetartion Testing Orlando*, *2*, 651–660.

Bolton, M. D., Gui, M. W., Garnier, J., Corte, J. F., Bagge, G., Laue, J., & Renzi, R. (1999). Centrifuge cone penetration tests in sand. *Géotechnique*, *49*(4), 543–552.

Carey, T., Gavras, A., Kutter, B., Haigh, S., Madabhushi, S., Okamura, M., ... Manzari, M. (2018). A new shared miniature cone penetrometer for centrifuge testing. In *Physical modelling in geotechnics* (pp. 293–298). Physical Modelling in Geotechnics. doi:10.1201/9780429438660-38

Coelho, P., Haigh, S., & Madabhushi, G. (2003). Boundary effects in dynamic centrifuge modelling of liquefaction in sand deposits.

DeJong, J. T., Frost, J. D., & Cargill, P. E. (2001). Effect of surface texturing on cpt friction sleeve measurements. *Journal of Geotechnical and Geoenvironmental Engineering*, *127*(2), 158–168. doi:10.1061/(ASCE)1090-0241(2001)127:2(158)

Elbrich, C. (1994). Pileless jacke foundations: A new era. *Offshore Engineering Society, British GEotechnical Society and Ground Engineering Joint Meeting.*

Fioravante, V. (2002). On the shaft friction modelling of non-displacement piles in sand. *Soils and Foundations*, *42*, 23–33. doi:10.3208/sandf.42.2_23

Ghayoomi, M., Jarast, P., Mirshekari, M., & Borghei, A. (2018). Application of cone penetrometer for unsaturated soils inside geotechnical centrifuge. *Proc. of the 7th International Conference on Unsaturated Soils.*

Gui, M., & Bolton, M. D. (1998). Geometry and scale effects in cpt and pile design.

Gui, M., Bolton, M. D., & Phillips, R. (1993). Review of miniature soil probes for model tests.

Jacobs, P. (2004). Cone penetration testing cpt. *Technical Report, Fugro Engineering Services Ltd.*

Jaeger, R., DeJong, J., Boulanger, R., Low, H. E., & Randolph, M. (2010). Variable penetration rate cpt in an intermediate soil.

Jamiolkowski, M., Presti, D. C. F. L., & Manassero, M. (2001). Evaluation of relative density and shear strength of sands from cpt and dmt. In *Soil behavior and soft ground construction* (pp. 201–238). doi:10.1061/40659(2003)7

Kim, J.-H., Kim, D.-J., Kim, D., & Choo, Y. W. (2013). Development of miniature cone and characteristics of cone tip resistance in centrifuge model tests. *Journal of The Korean Society of Civil Engineers*, *33*. doi:10.12652/Ksce.2013.33.2.631

Konkol, J. (2014). Derivation of the scaling laws used in geotechnical centrifuge modelling-application of dimensional analysis and buckingham π theorem. *Technical Sciences*, *17*, 31–44.

Lunne, T., Robertson, P., & Powell, J. (1997). *Cone penetration testing in geotechnical practice* (1st ed.). Blackie Academic and Professional, London.

Mo, P.-Q. (2014). Centrifuge modelling and analytical solutions for the cone penetration test in layered soils.

Nikudel, M., S.E., M., Khamehchiyan, M., & Jamshidi, A. (2012). Using miniature cone penetration test (mini-cpt) to determine engineering properties of sandy soils. *Journal of Geopersia*, 65–76.

Poulsen, R., Nielsen, B. N., & Ibsen, L. B. (2013). Correlation between cone penetration rate and measured cone penetration parameters in silty soils.

Salomon's Metalen B.V. (2016). The red book. Retrieved November 24, 2019, from https://salomons-metalen.com/images/general/salomon_catalog_2016.pdf

Schneider, J., Lehane, B., & Schnaid, F. (2007). Velocity effects on piezocone measurements in normally and over consolidated clays. *The International Journal of Physical Modelling in Geotechnics*, *7*(2), 23–34.

Schofield, A. N. (1980). Cambridge geotechnical centrifuge operations. *Géotechnique*, *30*(3), 227–268.

Taylor, R. (1994). Centrifuges in modelling: Principles and scale effects. (pp. 19–33). doi:10.1201/9781482269321-2

Wood, D. (2004). *Geotechnical modelling*. Spon Press.

List of Symbols

a	Acceleration
A	Area
d_{50}	Average Grain Size
R	Centrifuge Radius
c_v	Coefficient of Consolidation
q_c	Cone Resistance
D	Container Width/Diameter
ρ	Density
u	Displacement
σ'	Effective Stress
F	Force
M	Mass
D_M	Model Dimensions
N	Modelling Scale
Q	Normalized Cone Resistance
z_p	Normalized Penetration Depth
V	Normalized Velocity
z	Penetration Depth
B	Probe Diameter
D_P	Prototype Dimensions
f_s	Sleeve Friction
ϵ	Strain
σ	Total Stress
v	Velocity
γ	Volumetric Weight

Appendix

Appendix 1: Results from Tests Conducted with the Deltares ø7mm Miniature Cone

The tests were conducted at *1g* due to uncertainties with respect to measurement capabilities. As the data acquisition system used for this device was unknown, the wiring was connected to a voltmeter to obtain readings. Upon applying pressure on the cone tip, the voltage would decrease to the negative.

A series of sand samples were prepared in order to test this device. The relationship between the voltage readings and the tip resistance were obtained through calibration.

The device was initially calibrated in order to obtain a relationship between the registered voltage and applied forces. Illustrated in Figure 19, a linear relationship was obtained. The calibration was done by driving the CPT probe on top of a stack of paper sheets and applying forces and noting the corresponding voltage readings. The calibration data is summarized in Table 12.

Table 12: Calibration Data

F_v	-0.269	2.956	4.971	11.957	31
V	0.427	0.38899	0.332	0.223	-0.096

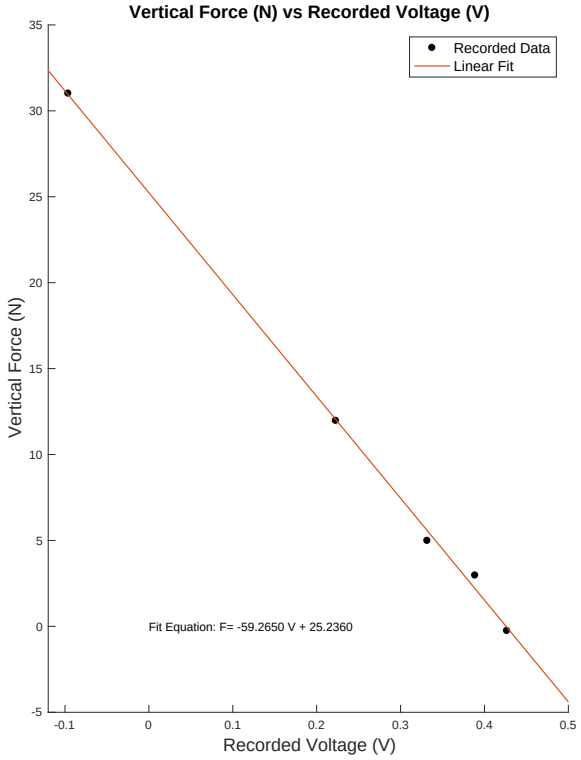

Figure 19: Calibration of Deltares ø8 mm Miniature CPT

As it can be seen the readings and the applied forces have a linear relationship. The resultant conversion equation is illustrated in equation 30.

$$F = -59.2650 \times V + 25.2360 \tag{30}$$

The specifications of the test are summarized in Table 13 and Figures 13 to 15 illustrate the obtained results.

Table 13: Specifications of Tests

Test	Sample Container Type	Soil Sample	g-Level
Test 1	Rectangular	Coarse Sand	1g
Test 2	Rectangular	Coarse Sand	1g
Test 3	Rectangular	Fine Sand	1g

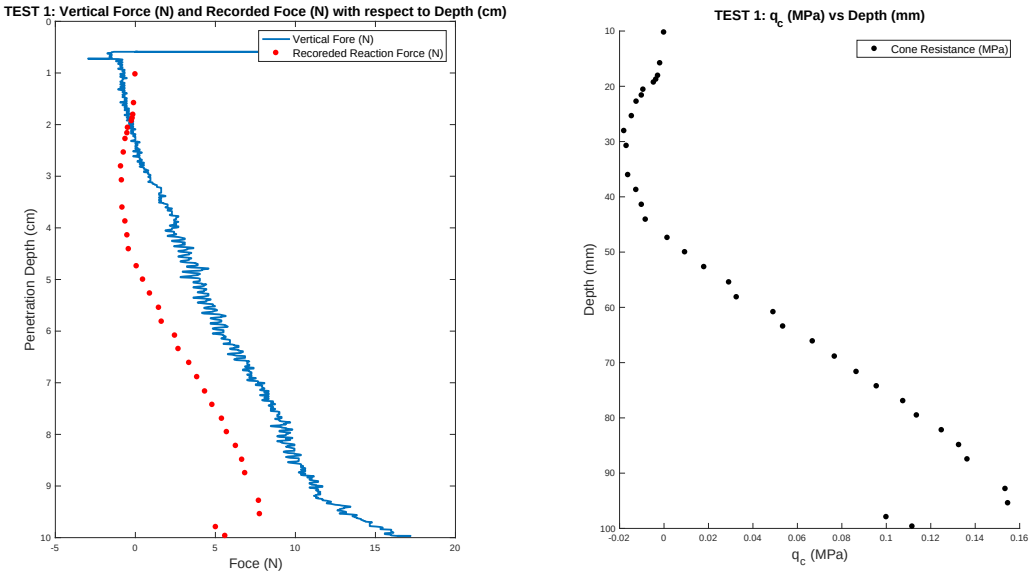

(a) Test 1: F_v (N) and F_{rv} (N) vs Depth (cm)

(b) Test 1: q_c (MPa) vs Depth (cm)

Figure 20: Test 1

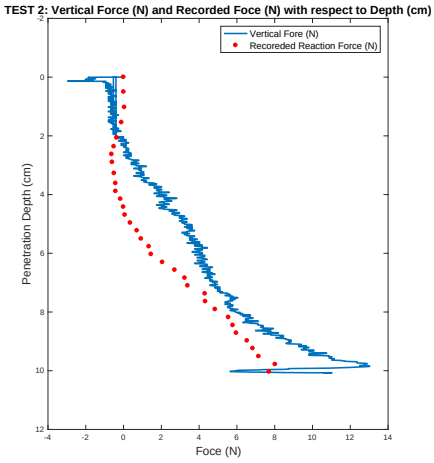

(a) Test 2: F_v (N) and F_{rv} (N) vs Depth (cm)

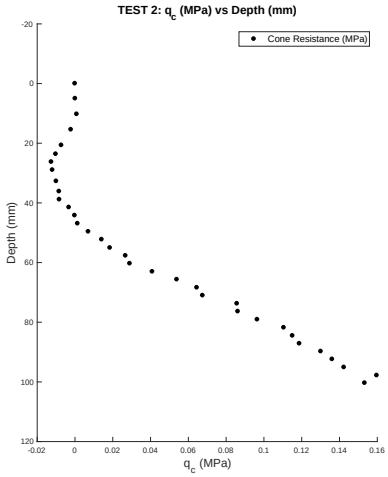

(b) Test 2: q_c (MPa) vs Depth (cm)

Figure 21: Test 2

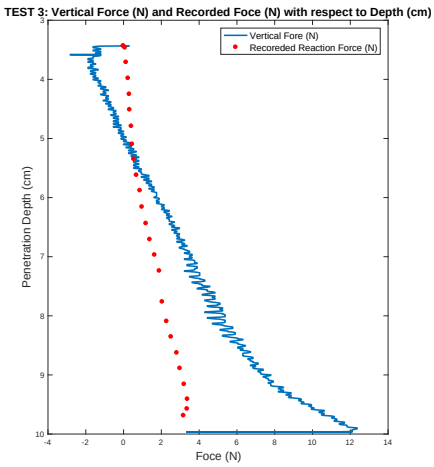

(a) Test 3: F_v (N) and F_{rv} (N) vs Depth (cm)

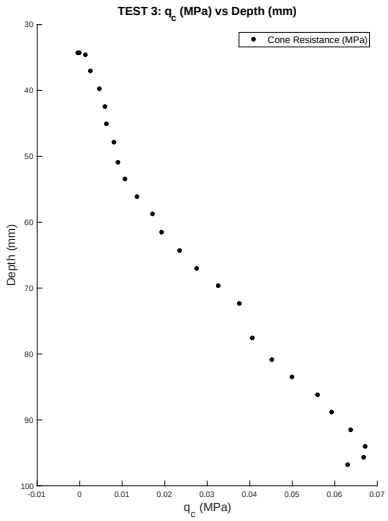

(b) Test 3: q_c (MPa) vs Depth (cm)

Figure 22: Test 3